Impact of the Arrangement of Shielding Material on the Efficiency of Dose Reduction for 252 Cf Neutron Radiation Sources using OpenMC code

ABDELHAMID JALIL[(1,*)], HOUDA ABBASSI[(1)], MOHAMMED HASSOUNI[(1)]

[(1)] Nuclear Centre of Energy, Science and Nuclear Techniques, Morocco

*Corresponding author: Abdelhamid JALIL, email address: jalilabdelhamid@gmail.com

Abstract

Neutrons are fundamental subatomic particles with diverse applications, including power generation, medical imaging, and national security. Safely harnessing nuclear and radioactive materials requires the selection of appropriate shielding materials. In this study, we investigated the impact of various shielding configurations on neutron radiation reduction using the OpenMC Monte Carlo code. The study introduces a gradient configuration where material fractions (polyethylene, B_4C, lead) vary spatially across shielding layers. This approach contrasts with conventional uniform mixtures and demonstrates superior performance, achieving a 13% reduction in total neutron flux and 67% lower photon dose rate compared to the reference configuration. Our findings aim to establish a comprehensive framework for evaluating and optimizing gradient materials to enhance shielding performance. This research has significant potential to revolutionize radiation protection, with applications in aerospace, healthcare, and various industrial sectors.

Keywords: OpenMC; gradient materials; Shielding; Neutron dose; gamma dose

1. Introduction

Fundamental subatomic particles and neutrons have unique properties that significantly influence their roles in nuclear physics and a variety of applications. Unlike protons, neutrons have electric neutrality and a mass of approximately one atomic mass unit (AMU). They are also stable within atomic nuclei and decay as free neutron. Strong and weak nuclear forces govern their interactions with matter, allowing for efficient material penetration. Finally, neutrons have a magnetic moment, albeit smaller than that of protons, which affects their behavior in a magnetic field. The reaction cross-sections for various nuclear reactions and the existence of different energy levels, such as thermal and fast neutron, further contribute to their role in nuclear physics and applications.[1]

A valuable neutron source for scientific studies, industrial use, and the medical domain is Californium-252. Because of its spontaneous nuclear fission, this radioactive isotope has been a helpful instrument for producing neutron since its discovery in 1950. Because of its unique properties, Californium-252 [2] is a valuable option for various applications, including material analysis, cancer treatment, and neutron radiography [3], [4].

In many scientific and industrial contexts, neutron shielding is essential for maintaining controlled environments and ensuring safety. Because neutrons are uncharged particles, it can be difficult to effectively contain them because they can quickly pierce objects. In this

situation, using shielding materials to lessen the effects of neutron radiation becomes essential [5], [6].

Effective neutron radiation shielding requires a carefully designed, multi-layered system. Unlike charged particles, neutrons are electrically neutral and interact unpredictably with matter, making them challenging to block. No single material can stop neutrons of all energy levels (thermal, epithermal, and fast) while avoiding secondary radiation or residual radioactivity. To address this, engineers and physicists combine materials with complementary properties into a layered structure[7], [8].

The first layer often consists of a moderator, such as hydrogen-rich polymers like polyethylene, epoxy, and polyamide are commonly used in shielding applications. Among these, high-density polyethylene (HDPE) stands out as a top choice is highly effective. Its high hydrogen content (~14%) makes it exceptionally effective at slowing neutrons through elastic scattering. In HDPE, hydrogen atoms interact with neutrons via the $^{1}H(n,\gamma)^{2}H$ reaction, which has a thermal neutron capture cross-section of 0.33 barns[9]. However, this reaction produces secondary 2.2 MeV gamma rays a drawback that requires additional shielding layers to block these energetic photons[10].

Next, a thermal neutron absorber is used. Common isotopes like boron-10 (^{10}B), lithium-6 (^{6}Li), or cadmium-113 (^{113}Cd) are embedded in this layer. These materials exploit nuclear reactions (n,α) and (n,γ) to capture neutrons[11].

A gamma-ray shield (e.g., lead, concrete, or steel) is then added to block secondary photons generated during neutron absorption. This layer ensures that residual gamma radiation does not pose a health or safety risk[8], [9].

The neutron behavior in complicated systems can be simulated using OpenMC, an open-source Monte Carlo particle transport algorithm that is strong and flexible. This computational tool, which was created by the Massachusetts Institute of Technology (MIT) and the OpenMC development team, has become well-known in the fields of nuclear engineering and physics for its accuracy and effectiveness in simulating neutron transport processes. OpenMC uses Monte Carlo techniques to simulate the random motion and interactions of neutron as they pass through various types of materials. Its capabilities cover a broad spectrum of applications such as radiation shielding, reactor physics, and nuclear criticality safety evaluations. [12].

The International Commission on Radiological Protection (ICRP) is an independent, nonprofit organization that aims to advance the science of radiological protection for public benefit. It provides recommendations and guidance on all aspects of protection against ionizing radiation, with the Main Commission serving as the governing body responsible for setting policies and providing general direction. [13].

2. Methodology

The geometry of the proposed neutron radiation shielding consists of three different materials: a moderator to slow down the neutron, a neutron absorber to absorb the slowed-down neutron, and a photon absorber introduced to absorb the gamma rays produced by the (n, gamma) reaction during the neutron absorption process. The materials used in this study were selected based on the characteristics of the formed isotopes. Light isotopes such as hydrogen (H) were chosen to thermalize neutron. Isotopes with high absorption cross-sections boron (B) were selected. Finally, heavier element lead (Pb) was chosen to attenuate the energy of the photon rays. In this study, we selected polyethylene (density: 0.93 g/cm^3) as the thermalizer, boron carbide (density: 2.52 g/cm^3) as the neutron absorber, and lead (density: 11.35 g/cm^3) as the attenuator of gamma rays[14], [15].

The shape of the shielding geometry set as a cubic with dimensions of 10 cm × 10 cm × 10 cm. The thicknesses of the moderator, neutron absorber, and photon absorber were 3.5, 1.5, and 5 cm, respectively. Six configurations of this arrangement were modeled, along with

uniform and gradient mixtures conserving the same total weight fraction of materials, we do not evaluate chemical reaction and stability in the mixite material we only focused on the performance in shielding, as detailed in **Table 1**.

Table 1: The representation of the different benchmarks of the shielding

Configuration	Plot Basis XZ
Configuration 1: Polyethene-B4C-Lead	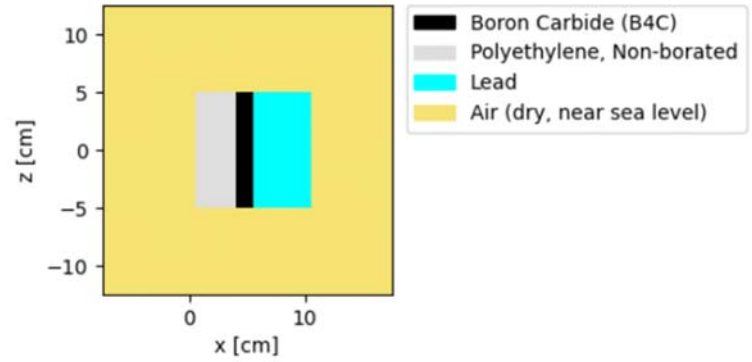
Configuration 2: B4C-Polyethene-Lead	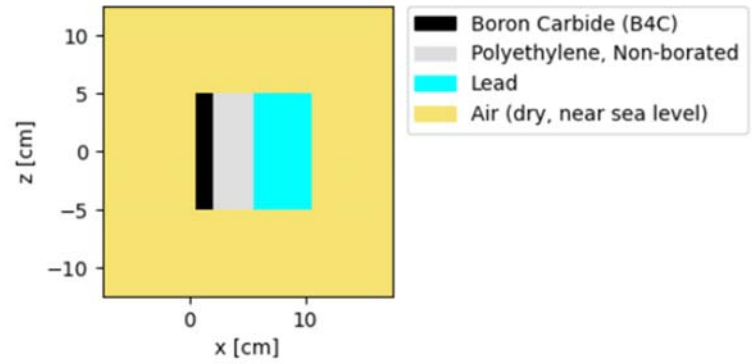
Configuration 3: Lead-B4C-Polyethene	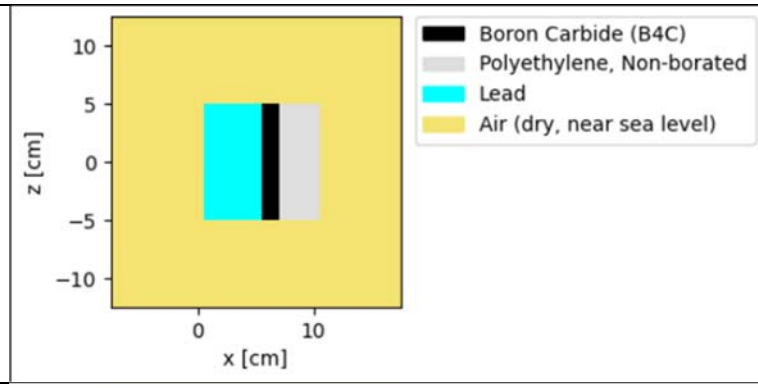
Configuration 4: Lead-Polyethene-B4C	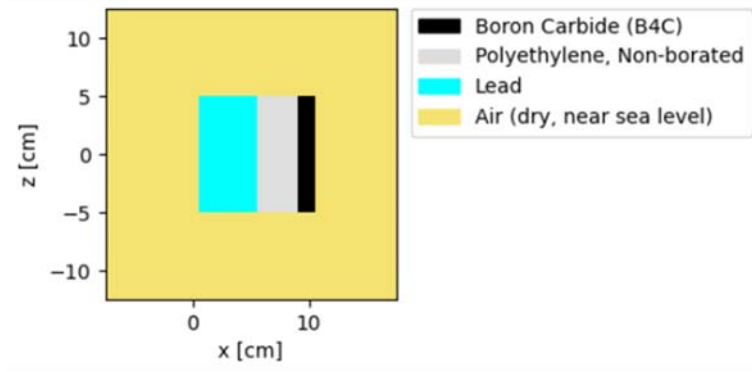

Configuration 5: Polyethene-Lead-B4C	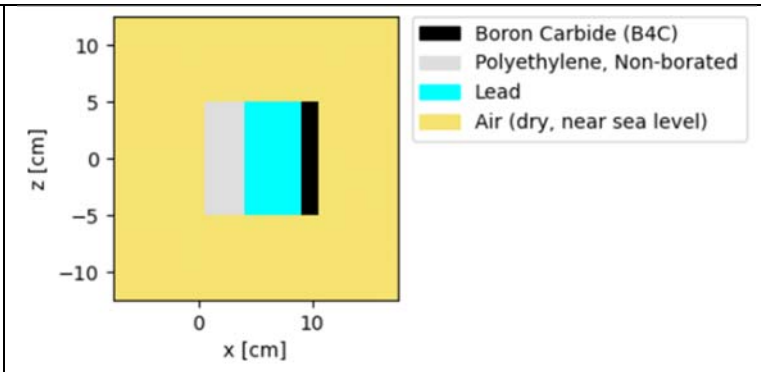
Configuration 6: B4C-Lead-Polyethene	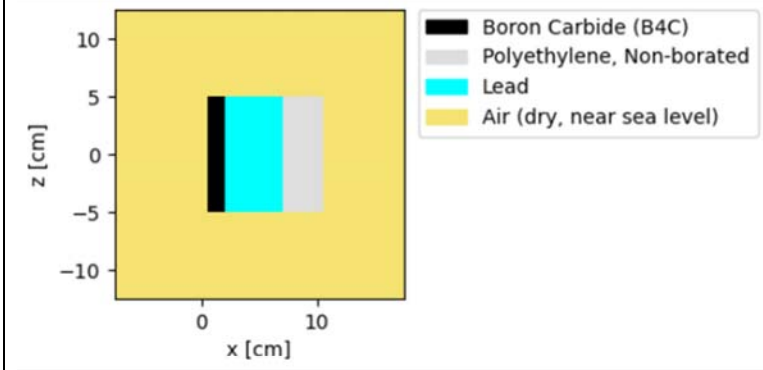
Configuration Uniform: - 35%[1] Polyethene - 15% Mirrobor - 50% Lead	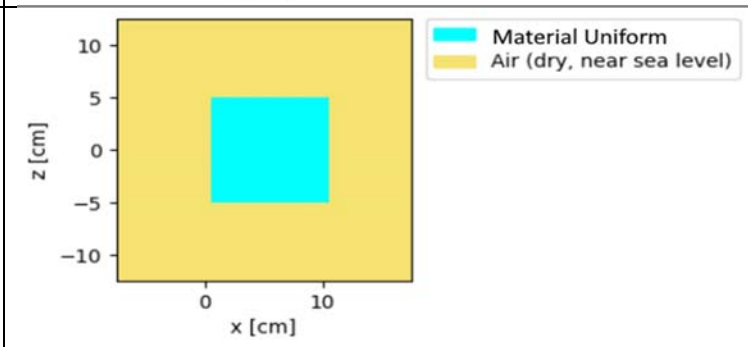
Configuration gradient:	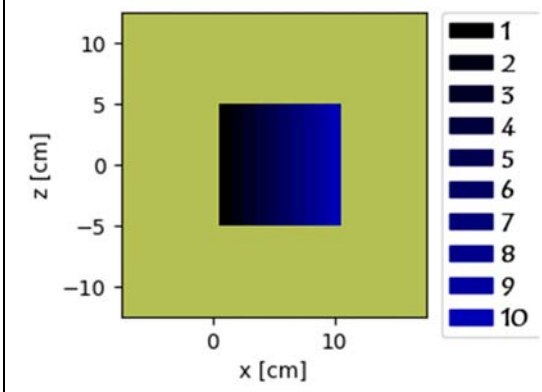

[1] Volume Fraction

LAYER	1	2	3	4	5	6	7	8	9	10
POLYETHENE %	100	100	60	20	60	10	0	0	0	0
B4C %	0	0	10	40	20	80	0	0	0	0
LEAD %	0	0	30	40	20	10	100	100	100	100

This study was performed using the Monte Carlo code OpenMC version 15.0 coupled with the ENDF-VII.1 cross-section data of neutron and photons. The source was sited 0.5 cm from the frontal side of the shielding. The neutron spectrum was modeled in OpenMC using the built-in Watt fission **(equation 1)** spectrum for 252 Cf [4], where is the normalization constant, a = 1.18MeV, and b = 1.03419MeV-1 [16](figure 1).

$$p(E)dE = ce^{-\frac{E}{a}}\sinh(bE)\,dE \quad (1)$$

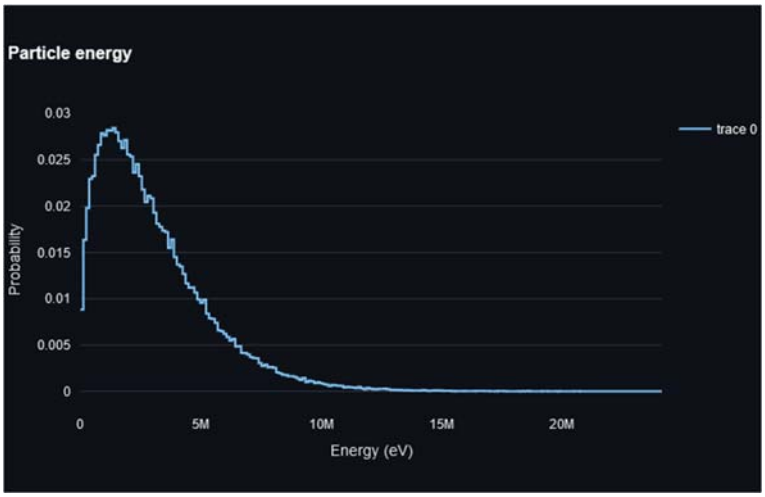

Figure 1: Source plot of the 252Cf probability function of Watt fission with 1000 samples.

Utilizing a single material for shielding instead of a series of materials reduces the complexity of the laboratory setting. i.e. For each material used in the laboratory, various measures must be taken into consideration, including chemical and physical considerations.

To evaluate the composition of the neutron flux in the presence of a shielding instrument, three neutron energy ranges were determined: thermal (0.025 eV – 1 eV), epithermal (1 eV – 100 keV), and fast (100 keV – 10 MeV)[17]. In addition, the neutron and photon doses [13] were calculated in a sphere containing tissue material [15] (A tissue-equivalent material (density: 1.0 g/cm³; atomic fractions: 76.2% O, 11.1% C, 10.1% H, 2.6% N) was used to calculate dose rates.) using effective dose conversion coefficients from ICRP-116[18].

2. Results and discussions

The results of the simulations for various configurations of the arrangement of shielding materials, as outlined in Table 1. The output provides a breakdown of three energy components: thermal, epithermal, and rapid. These specific quantities were selected because of their ability to accurately reflect the capabilities of isotopes in shielding against neutron sources.

Table 2 presents flux values (in n/cm.s per particle source) across different configurations. This data illustrates the neutron flux across different energy ranges (thermal, epithermal,

rapid) as well as the total flux for each configuration. Notably, configurations with different shielding arrangements exhibit varied flux values, suggesting the impact of shielding materials on neutron flux. Changing the order of shielding materials results in a significant change in the output neutron flux. Meanwhile, the arrangement of the moderator and neutron absorber significantly influences the outcome. Configuration 1 is used as a reference, with a performance ratio set to 1.00. Configurations Configuration 5 and Configuration gradient exhibit the best overall results, with ratios of 0.87, indicating superior efficiency in reducing the total neutron flux. In contrast, Configuration 6 has the highest ratio (1.49), suggesting relatively poor shielding performance.

For configurations 1, 4, and 5, where the moderator is placed before the neutron absorber, the flux values are notably lower, around 50%, compared with configurations 2, 3, and 6 (Figure 3).

Table 2:Flux with shielding materials in different configurations.

Configuration	**Thermal (Value ± Std)**	**Epithermal (Value ± Std)**	**Fast (Value ± Std)**	**Total (Value ± Std)**	**Ratio [2]**
Configuration 1	1.13E-05 ± 2.57E-06	9.80E-04 ± 2.35E-05	3.33E-02 ± 1.56E-04	3.43E-02 ± 6.05E-05	1
Configuration 2	6.69E-03 ± 6.84E-05	6.59E-03 ± 6.70E-05	3.15E-02 ± 1.52E-04	4.48E-02 ± 9.59E-05	1.31
Configuration 3	6.06E-03 ± 7.00E-05	7.23E-03 ± 6.59E-05	3.33E-02 ± 1.58E-04	4.66E-02 ± 9.80E-05	1.36
Configuration 4	7.20E-06 ± 2.27E-06	1.05E-03 ± 2.32E-05	2.98E-02 ± 1.44E-04	3.08E-02 ± 5.66E-05	0.90
Configuration 5	1.05E-05 ± 2.52E-06	1.01E-03 ± 2.64E-05	2.88E-02 ± 1.60E-04	2.98E-02 ± 6.31E-05	0.87
Configuration 6	7.39E-03 ± 6.62E-05	7.97E-03 ± 7.04E-05	3.58E-02 ± 1.51E-04	5.11E-02 ± 9.59E-05	1.49
Configuration Uniform	4.87E-05 ± 5.32E-06	3.37E-03 ± 5.06E-05	3.16E-02 ± 1.54E-04	3.50E-02 ± 6.98E-05	1.02
Configuration gradient	9.06E-06 ± 2.78E-06	1.34E-03 ± 3.08E-05	2.85E-02 ± 1.41E-04	2.99E-02 ± 5.82E-05	0.87
without_ shielding	2.10E-07 ± 9.88E-08	4.01E-05 ± 1.37E-06	9.68E-02 ± 9.26E-05	9.68E-02 ± 3.14E-05	2,82

[2] Configuration (i) / configuration 1

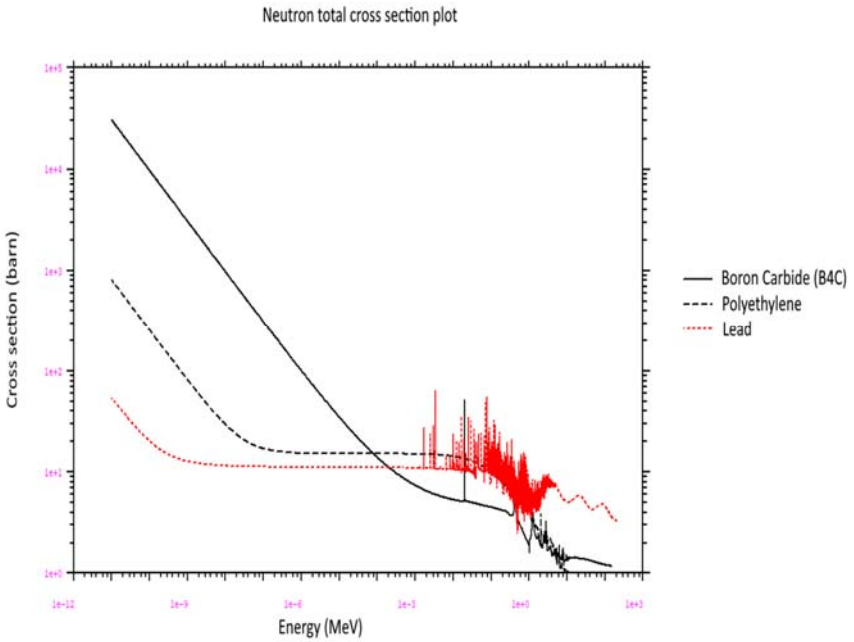

Figure 2: Total neutron cross section Boron carbide, Polyethylene and Lead (Barn)

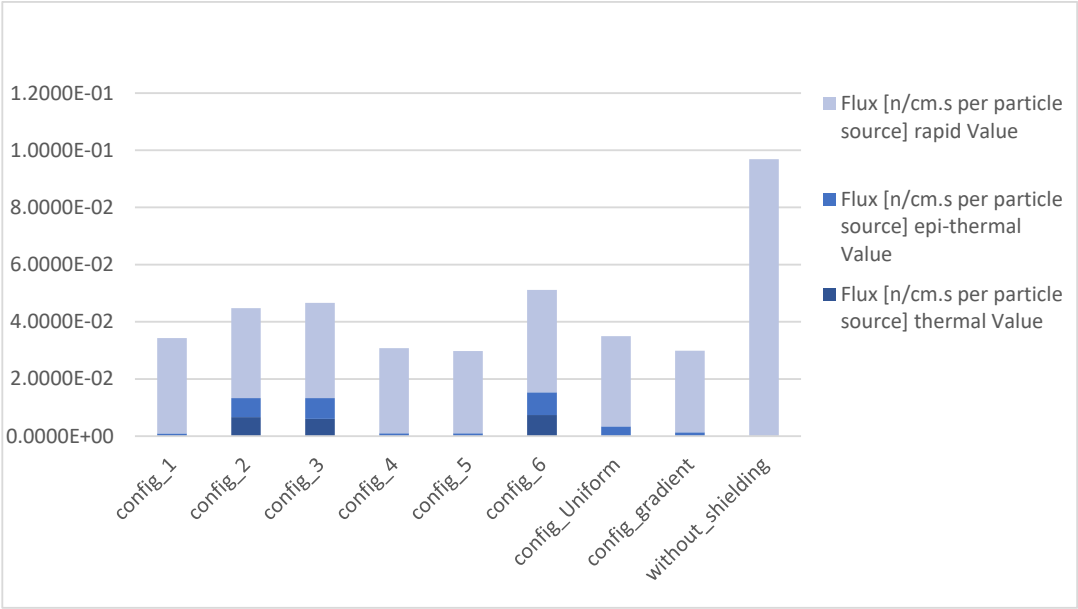

Figure 3: Composition of neutron flux without shielding and with different shielding configurations

The photon absorber Lead practically exhibits no effect on neutron moderation or absorption (configurations 2, 3, and 6) due to its neutron cross-section characteristics compared to polyethylene and boron carbide (Figure 2). However, in the epithermal range containing a dense resonance peak, this will impact neutron transport in this region.

For neutron flux shielding, configuration 5 and gradient shows the best performance for the overall neutron energy range. In addition, it has a lower ratio by configuration 1 in total

flux value by 0.87%. Lastly, the uniform configuration had a similar performance for the configuration 1 (Table 2 & Figure 3).

Unfortunately, when shielding against neutron radiation, other particles/radiation may be present as a result of the interaction with matter. Gamma is one of the hardest in shielding of those particles. As part of this study, we evaluated the neutron and gamma dose rates to determine the best-performing shielding configuration.

The dose rates of neutron and gamma were calculated using integrated coefficient values publication 116 are shown in (Table 3). These quantities were calculated at the exit of the shielding, and the composition of the tissue-equivalent material used to calculate.

In the case of the traditional configuration, Configuration 1 (moderator, neutron absorber, and photon absorber) exhibits the best performance. The dose rate conversion factors are related to the energy of the neutron. i.e. low-energy neutrons (thermal and epithermal) tend to have higher dose conversion factors because they are more likely to be captured by nuclei in biological tissues, leading to secondary radiation that can cause significant biological damage. While the high-energy neutrons (fast neutrons) have lower dose conversion factors compared to low-energy neutrons, they can penetrate deeper into tissue and cause direct ionization along their path[19]. This is reflected in the neutron dose rate being lowest for the configuration with the lowest thermal and epithermal neutron flux (configuration 1), even when compared with the configuration that has the lowest total neutron flux (configuration 5). In addition of the performance in neutron dose reduction, configuration 1 Also provide the best performance for photon dose rate reduction between the six configurations.

Table 3:Neutron dose rate and Photon dose rate per source particle [Sv/h]

configuration	Neutron dose rate [Sv/h] per particle source		Photon dose rate [Sv/h] per particle source		Neutron dose rate ratio[3]	Photon dose rate ratio
	value	Std	value	Std		
Config 1	1.32E-14	±8.03E-17	4.01E-18	±2.78E-19	1.00	1.00
Config 2	1.47E-14	±9.07E-17	7.78E-18	±3.65E-19	1.12	1.94
Config 3	1.50E-14	±8.31E-17	3.15E-17	±5.94E-19	1.14	7.86
Config 4	1.42E-14	±7.59E-17	6.59E-17	±7.86E-19	1.08	16.42
Config 5	1.33E-14	±8.32E-17	5.75E-17	±5.87E-19	1.01	14.33
Config 6	1.56E-14	±8.01E-17	1.78E-17	±5.24E-19	1.19	4.44
Config Uniform	1.39E-14	±7.75E-17	7.76E-18	±2.51E-19	1.06	1.93
Config gradient	1.31E-14	±7.50E-17	1.34E-18	±1.63E-19	0.99	0.33

The neutron and photon radiation pass through a uniform configuration with a ratio dose rate 1.06 and 1.96 higher compared to configuration 1. However, in the last configuration, the gradient configuration shows promising results with ratio dose rate values 0.99 lower for neutrons and 0.33 lower for photons compared to configuration reference number 1.

[3] Configuration (i) / configuration 1

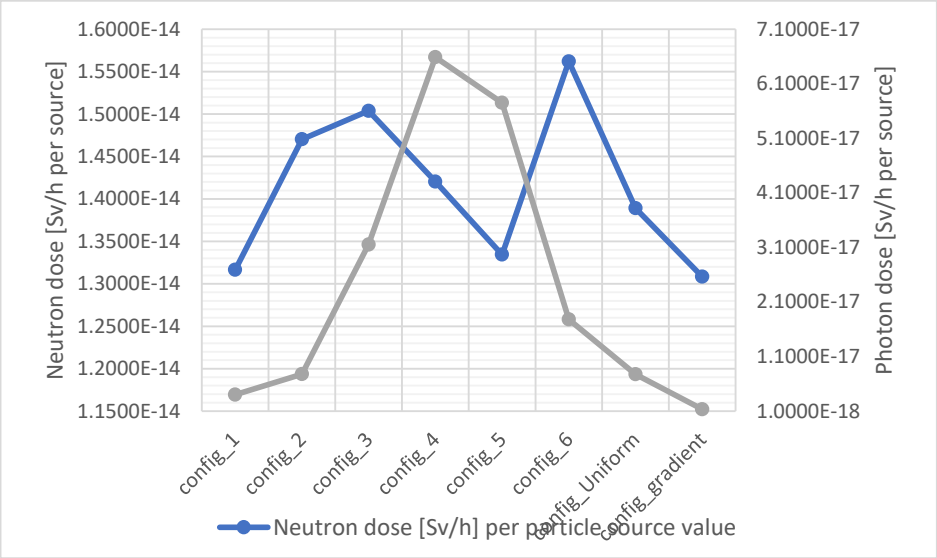

Figure 4: Dose rate for neutron and photons produced by the interaction of neutron material for different configurations.

3. Conclusion

The study concludes that the arrangement of shielding materials significantly influences the shielding effectiveness for neutron and gamma radiation. Configurations where the neutron absorber (B_4C) is positioned last minimize thermal and epithermal neutron flux leakage. Among the tested setups, the gradient configuration provided the best overall shielding performance, achieving the lowest rapid neutron flux and reduced dose rates for both neutrons and photons.

This work highlights the importance of material selection and arrangement in designing effective radiation shielding, with applications in fields such as nuclear reactors, medical facilities, and industrial neutron sources.

Future research will focus on the chemical integrity and stability of the proposed shielding materials. While the current study emphasizes their physical and radiological performance, further investigations are needed to understand their chemical behavior. Additionally, studies on the fabrication processes for gradient materials and the influence of chemical stability on shielding effectiveness will be essential for translating these findings into practical applications.

Conflict of Interest

The authors declare that there is no conflict of interest with respect to the publication of this article

References

[1] I. Obodovskiy, “Interaction of Neutrons With Matter,” in *Radiation*, Elsevier, 2019, pp. 151–160. doi: 10.1016/B978-0-444-63979-0.00007-0.

[2] X. Liu, Y. Shi, and J. Li, “Time-dependent multiplicity for Cf-252 neutron source,” *Applied Radiation and Isotopes*, vol. 199, p. 110836, Sep. 2023, doi: 10.1016/J.APRADISO.2023.110836.

[3] B. C. Anderson, K. E. Holbert, and H. Bowler, “Design, Construction, and Modeling of a 252Cf Neutron Irradiator,” *Science and Technology of Nuclear Installations*, vol. 2016, 2016, doi: 10.1155/2016/9012747.

[4] F. D. Becchetti, M. Febbraro, R. Torres-Isea, M. Ojaruega, and L. Baum, “252Cf fission-neutron spectrum using a simplified time-of-flight setup: An advanced teaching laboratory experiment,” *Am J Phys*, vol. 81, no. 2, pp. 112–119, Feb. 2013, doi: 10.1119/1.4769032.

[5] H. Amsil *et al.*, “Conceptual implementation stages for Moroccan PGAA/NI instruments: STAGE i & II,” *Journal of Neutron Research*, vol. 22, no. 4, pp. 403–415, 2020, doi: 10.3233/JNR-200171.

[6] S. Ahmad, B. Chang, C. Lian, S. A. Raza, and M. Wang, “Design and development study of gradient composite shielding material for nuclear radiation,” *Nuclear Engineering and Design*, vol. 414, Dec. 2023, doi: 10.1016/j.nucengdes.2023.112517.

[7] K. N. Leung, “New mini neutron tubes for oil well logging applications,” *Applied Radiation and Isotopes*, vol. 221, p. 111798, Jul. 2025, doi: 10.1016/J.APRADISO.2025.111798.

[8] S. Verma and A. Kumar Srivastava, “ADVANCED RADIATION SHIELDING MATERIALS,” 2024.

[9] S. T. Abdulrahman, Z. Ahmad, S. Thomas, and A. A. Rahman, “Introduction to neutron-shielding materials,” *Micro and Nanostructured Composite Materials for Neutron Shielding Applications*, pp. 1–23, Jan. 2020, doi: 10.1016/B978-0-12-819459-1.00001-5.

[10] A. M. El-Khayatt, “Calculation of photon shielding properties for some neutron shielding materials,” *Nuclear Science and Techniques*, vol. 28, no. 5, p. 69, 2017, doi: 10.1007/s41365-017-0222-y.

[11] D. R. Mcalister, “Neutron Shielding Materials Revision 2.1,” 2016.

[12] P. K. Romano, N. E. Horelik, B. R. Herman, A. G. Nelson, B. Forget, and K. Smith, “OpenMC: A state-of-the-art Monte Carlo code for research and development,” *Ann Nucl Energy*, vol. 82, pp. 90–97, 2015, doi: https://doi.org/10.1016/j.anucene.2014.07.048.

[13] C. H. Clement *et al.*, “Annals of the ICRP Conversion Coefficients for Radiological Protection Quantities for External Radiation Exposures The International Commission on Radiological Protection and The International Commission on Radiation Units and Measurements.”

[14] M. Mitev, D. Dimitrov, Z. Zahariev, and A. Naydenov, “Investigation of an Innovative Material for Neutron Shielding,” vol. 22, no. 1, pp. 38–41, 2017.

[15] R. J. McConn Jr, C. J. Gesh, R. T. Pagh, R. A. Rucker, and R. G. Williams III, “Compendium of Material Composition Data for Radiation Transport Modeling - Revision 1, PIET-43741-TM963, PNNL-15870 Rev. 1,” 2011, [Online]. Available: http://www.pnnl.gov/main/publications/external/technical_reports/PNNL-15870Rev1.pdf

[16] J. Armstrong *et al.*, “User’s Manual Code Version 6.2”.

[17] A. Jalil *et al.*, “Determining PGAA collimator plug design using Monte Carlo simulation,” *Nuclear Engineering and Technology*, vol. 53, no. 3, pp. 942–948, 2021, doi: 10.1016/j.net.2020.08.016.

[18] N. Petoussi-Henss *et al.*, “Conversion Coefficients for Radiological Protection Quantities for External Radiation Exposures,” *Ann ICRP*, vol. 40, no. 2–5, pp. 1–257, 2010, doi: 10.1016/j.icrp.2011.10.001.

[19] Icrp, “Annals of the ICRP Published on behalf of the International Commission on Radiological Protection.”